AMERICAN SOCIETY FOR MICROBIOLOGY | Journal of Virology

| Editor's Pick | Virology | Full-Length Text

The membrane-associated ubiquitin ligase MARCHF8 stabilizes the human papillomavirus oncoprotein E7 by degrading CUL1 and UBE2L3 in head and neck cancer

Mohamed I. Khalil,[1,2] Canchai Yang,[1] Lexi Vu,[1] Smriti Chadha,[1] Harrison Nabors,[1] Claire D. James,[3] Iain M. Morgan,[3] Dohun Pyeon[1]

AUTHOR AFFILIATIONS See affiliation list on p. 16.

ABSTRACT The human papillomavirus (HPV) oncoprotein E7 is a relatively short-lived protein required for HPV-driven cancer development and maintenance. E7 is degraded through ubiquitination mediated by cullin 1 (CUL1) and the ubiquitin-conjugating enzyme E2 L3 (UBE2L3). However, E7 proteins are maintained at high levels in most HPV-positive cancer cells. A previous proteomics study has shown that UBE2L3 and CUL1 protein levels are increased by the knockdown of the E3 ubiquitin ligase membrane-associated ring-CH-type finger 8 (MARCHF8). We have recently demonstrated that HPV16 upregulates MARCHF8 expression in HPV-positive keratinocytes and head and neck cancer (HPV+ HNC) cells. Here, we report that MARCHF8 stabilizes the HPV16 E7 protein by degrading the components of the S-phase kinase-associated protein 1-CUL1-F-box ubiquitin ligase complex in HPV+ HNC cells. We found that *MARCHF8* knockdown in HPV+ HNC cells drastically decreases the HPV16 E7 protein level while increasing the CUL1 and UBE2L3 protein levels. We further revealed that the MARCHF8 protein binds to and ubiquitinates CUL1 and UBE2L3 proteins and that MARCHF8 knockdown enhances the ubiquitination of the HPV16 E7 protein. Conversely, the overexpression of CUL1 and UBE2L3 in HPV+ HNC cells decreases HPV16 E7 protein levels and suppresses tumor growth *in vivo*. Our findings suggest that HPV-induced MARCHF8 prevents the degradation of the HPV16 E7 protein in HPV+ HNC cells by ubiquitinating and degrading CUL1 and UBE2L3 proteins.

IMPORTANCE Since human papillomavirus (HPV) oncoprotein E7 is essential for virus replication; HPV has to maintain high levels of E7 expression in HPV-infected cells. However, HPV E7 can be efficiently ubiquitinated by a ubiquitin ligase and degraded by proteasomes in the host cell. Mechanistically, the E3 ubiquitin ligase complex cullin 1 (CUL1) and ubiquitin-conjugating enzyme E2 L3 (UBE2L3) components play an essential role in E7 ubiquitination and degradation. Here, we show that the membrane ubiquitin ligase membrane-associated ring-CH-type finger 8 (MARCHF8) induced by HPV16 E6 stabilizes the E7 protein by degrading CUL1 and UBE2L3 and blocking E7 degradation through proteasomes. MARCHF8 knockout restores CUL1 and UBE2L3 expression, decreasing E7 protein levels and inhibiting the proliferation of HPV-positive cancer cells. Additionally, overexpression of CUL1 or UBE2L3 decreases E7 protein levels and suppresses *in vivo* tumor growth. Our results suggest that HPV16 maintains high E7 protein levels in the host cell by inducing MARCHF8, which may be critical for cell proliferation and tumorigenesis.

KEYWORDS papillomavirus, HPV, E7, ubiquitination, E3 ligase, MARCHF8, MARCH8, head and neck cancer

Editor Koenraad van Doorslaer, College of Agriculture & Life Sciences, University of Arizona, Tucson, Arizona, USA

Address correspondence to Dohun Pyeon, dpyeon@msu.edu, or Mohamed I. Khalil, khalilm5@msu.edu.

The authors declare no conflict of interest.

See the funding table on p. 16.

Received 2 November 2023
Accepted 15 December 2023
Published 16 January 2024

Human papillomaviruses (HPVs) are non-enveloped DNA viruses that infect skin keratinocytes (1). The high-risk HPV genotypes such as HPV16 and HPV18 are causally associated with over 95% of cervical cancers, 25% of head and neck cancers (HNC), and most anogenital cancers (2, 3). High-risk HPV E6 and E7 interact with various cellular proteins to modulate almost all oncogenic mechanisms defined as cancer hallmarks (4). Thus, HPV-driven cancers are addicted to E6 and E7 expression, and their survival requires sustaining high E7 expression (5–7).

HPV16 E6 and E7 facilitate the ubiquitination and degradation of various host proteins by interacting with E2 ubiquitin-conjugating enzymes and E3 ubiquitin ligases (8–12). While E6 degrades p53 through E6AP, E7 degrades host proteins such as pocket proteins (pRb, p107, and p130) and the tyrosine-protein phosphatase non-receptor type 14 (PTPN14) through the cullin-RING E3 ubiquitin ligase complex (13–16). On the other hand, the HPV16 E7 protein is also degraded through ubiquitination by the S-phase kinase-associated protein (SKP)-Cullin-F box (SCF) ubiquitin ligase complex containing ubiquitin-conjugating enzyme E2 L3 (UBE2L3, also called UBCH7), cullin 1 (CUL1), and S-phase kinase-associated protein 2 (SKP2) (17). The SCF ubiquitin ligase complex ubiquitinates many cell cycle regulatory proteins, such as E2F1, p27, origin recognition complex subunit 1, and cyclin D1 (18–21). UBE2L3 interacts with various E3 ligases containing HECT (homologous of E6AP C-terminus) or RING (Really Interesting New Gene) finger domains (22, 23). Following SCF-mediated ubiquitination, E7 is degraded via the 26S proteasome (17, 24). Despite the efficient degradation mechanism in host cells, HPV-positive (HPV+) cancer cells maintain high levels of E7 proteins. Previous studies have shown that the E7 protein is stabilized by various mechanisms, such as deubiquitination (25) and phosphorylation (26). However, little is known about how the E7 protein overcomes its degradation by the SCF ubiquitin ligase complex-mediated ubiquitination in HPV+ cancer cells.

A recent study showed that membrane-associated ring-CH-type finger 8 (MARCHF8) knockdown in esophageal squamous cell carcinoma cells increases the levels of CUL1 and UBE2L3 proteins (27). MARCHF8 is a member of the MARCHF family of E3 ubiquitin ligases, which ubiquitinates diverse immune receptors, such as major histocompatibility complexes (MHC-I and MHC-II) (28, 29) and interleukin-1 (IL-1) receptor accessory protein (IL1RAP) (30). We have recently revealed that MARCHF8 is significantly upregulated in HPV+ HNC cells and inhibits apoptosis by ubiquitinating and degrading the death receptors from the tumor necrosis factor (TNF) receptor superfamily, Fas cell surface death receptor (FAS), and TNF-related apoptosis-inducing ligand receptors 1 and 2 (TRAIL-R1 and TRAIL-R2) (31).

Here, we show that MARCHF8 binds to and ubiquitinates CUL1 and UBE2L3 proteins in HPV+ HNC cells. Furthermore, knockdown or knockout of *MARCHF8* in HPV+ HNC cells significantly increased CUL1 and UBE2L3 protein levels, decreasing the levels of HPV16 E7 protein. Conversely, overexpression of CUL1 and UBE2L3 in HPV+ HNC cells decreases HPV16 E7 protein levels and suppresses tumor growth *in vivo*. These findings suggest that HPV-induced MARCHF8 stabilizes HPV16 E7 proteins to maintain the high levels of E7 in HPV+ HNC cells.

RESULTS

CUL1 and UBE2L3 overexpression increases the ubiquitination and decreases the HPV16 E7 protein levels in HPV+ HNC cells

HPV E7 was previously shown to be ubiquitinated and degraded by CUL1 and UBE2L3 in cervical cancer cells (17) (Fig. 1A). Hence, to examine if CUL1 and UBE2L3 enhance ubiquitination and degradation of HPV16 E7 protein in the HPV+ HNC cells, we generated SCC152 and SCC2 cells overexpressing CUL1 or UBE2L3 using lentiviral transduction and blasticidin selection. Western blotting showed that *CUL1* or *UBE2L3* overexpression significantly decreased HPV16 E7 protein levels in SCC152 (Fig. 1B and C) and SCC2 (Fig. 1D and E) cells. These results confirm that CUL1 and UBE2L3 reduce HPV16 E7 protein levels. Interestingly, CUL1 overexpression increased UBE2L3 protein

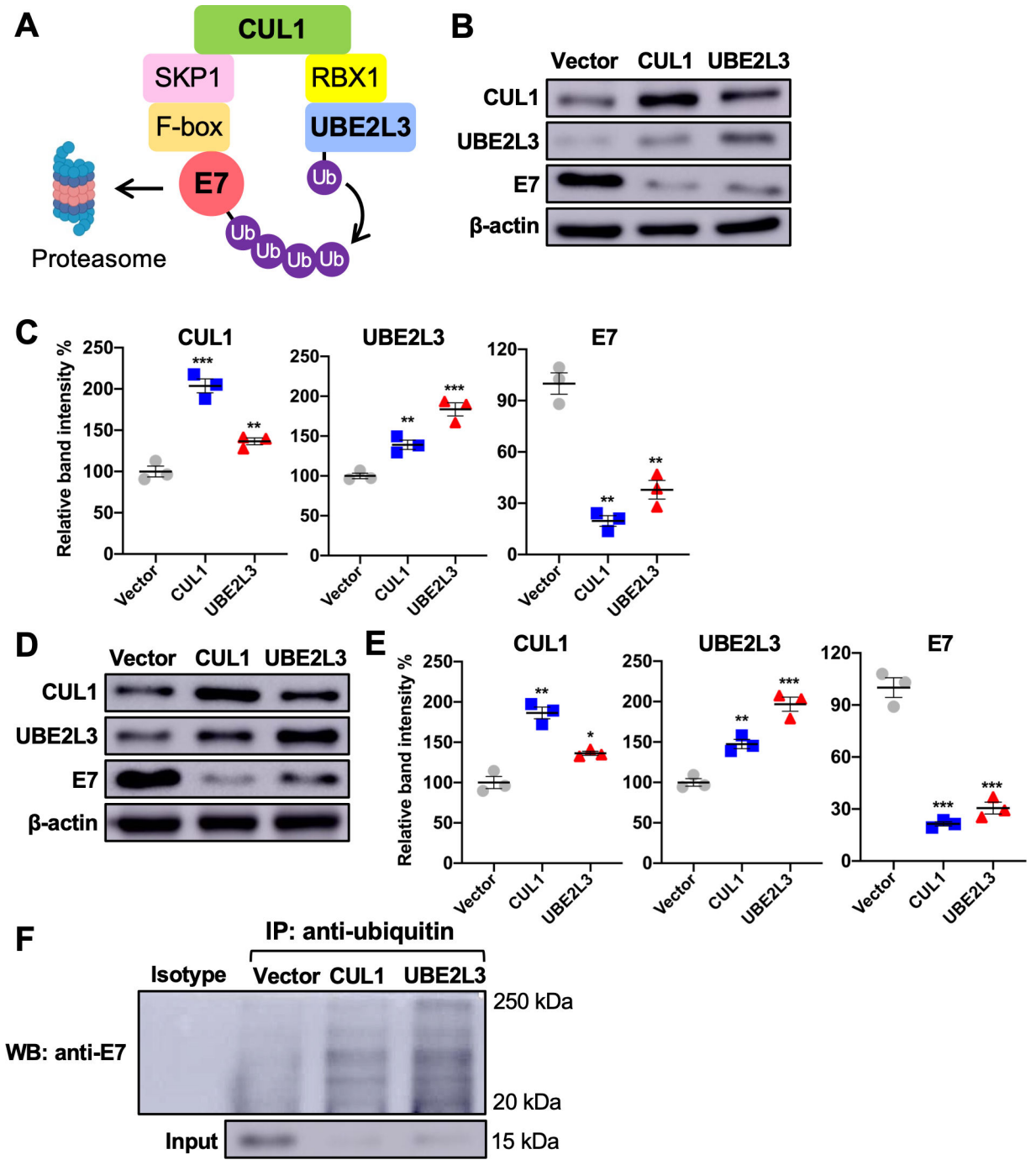

FIG 1 CUL1 and UBE2L3 overexpression increases the ubiquitination and decreases HPV16 E7 protein level in HPV+ HNC cells. (A) The schematic model of HPV16 E7 degradation through CUL1- and UBE2L3-mediated ubiquitination. Figure generated with a Biorender icon. CUL1 or UBE2L3 is overexpressed in HPV+ HNC (SCC152) (B–C) and SCC2 (D–E) cells using lentiviral transduction. CUL1, UBE2L3, HPV16 E7, and MARCHF8 proteins were detected by western blotting. The relative band intensities were quantified using NIH ImageJ in SCC152 (C) and SCC2 (E). β-Actin was used as an internal control. (F) SCC152 cells with CUL1 or UBE2L3 overexpression were treated with MG132 (10 µM). Ubiquitinated proteins were pulled down from the cell lysate using anti-ubiquitin antibody-conjugated magnetic beads, and HPV16 E7 protein was detected by western blotting. The data shown are means ± SD of three independent experiments. Student's *t*-test was used to determine *P*-values. $^{*}P < 0.05$, $^{**}P < 0.01$, $^{***}P < 0.001$.

levels in SCC152 and SCC2, and UBE2L3 overexpression increased CUL1 protein levels in the two cell lines. Next, to determine if CUL1 and UBE2L3 overexpression enhances the ubiquitination of HPV16 E7 proteins, we pulled down ubiquitinated proteins in whole

cell lysates from the proteasome inhibitor MG132-treated SCC152 cells overexpressing CUL1 or UBE2L3 using anti-ubiquitin antibody-conjugated magnetic beads. The results showed that ubiquitination levels of E7 (Fig. 1F) were increased by CUL1 and UBE2L3 overexpression in SCC152 cells despite the significantly lower levels of input E7 proteins compared to SCC152 cells with vector. These results suggest that CUL1 and UBE2L3 enhance HPV16 E7 ubiquitination and degradation.

CUL1 and UBE2L3 expression is downregulated in HPV+ HNC cells

To determine if HPV alters the endogenous CUL1 and UBE2L3 expression, we measured CUL1 and UBE2L3 protein levels in HPV+ HNC cells (SCC2, SCC90, and SCC152) compared to HPV- HNC cells (SCC1, SCC9, and SCC19) and normal keratinocytes (N/Tert-1) by western blotting. The results showed that CUL1 and UBE2L3 protein levels are significantly lower in HPV+ HNC cells compared to HPV− HNC cells and normal keratinocytes (Fig. 2A and B). To examine if CUL1 and UBE2L3 expression is transcriptionally regulated in HPV+ HNC cells, we measured CUL1 and UBE2L3 mRNA levels in HPV+ and HPV− HNC cells along with N/Tert-1 cells by reverse transcription-quantitative PCR (RT-qPCR). Our results showed that CUL1 mRNA expression was not significantly changed in SCC90 and SCC152 cells but upregulated in SCC2 cells compared to N/Tert-1 cells (Fig. 2C). On the other hand, UBE2L3 mRNA expression was significantly upregulated in all HPV+ HNC cells but downregulated in all HPV− HNC cells compared to N/Tert-1 cells (Fig. 2C). Additionally, our patient data from the previous study (2) revealed that CUL1 and UBE2L3 mRNA levels are consistently increased in HPV+ HNC patients compared to normal samples, while HPV− HNC patients also showed upregulation of CUL1 and UBE2L3 mRNA (Fig. 2D). These results suggest that the low CUL1 and UBE2L3 protein levels in HPV+ HNC cells are not caused by transcriptional regulation. However, another data set from TCGA indicates a possible decrease in CUL1 mRNA expression (THInCR.ca); it cannot be completely ruled out that CUL1 is also transcriptionally regulated.

To determine if proteasome-dependent protein degradation causes the low CUL1 and UBE2L3 protein levels in HPV+ HNC cells, CUL1 and UBE2L3 protein levels were measured in MG132-treated SCC152 cells. The results showed that MG132 treatment increased the CUL1 and UBE2L3 protein levels in SCC152 cells (Fig. 2E and F). These results suggest that the proteasome-dependent degradation of CUL1 and UBE2L3 proteins is enhanced in HPV+ HNC cells. Surprisingly, the HPV16 E7 protein level was not increased by MG132 treatment in the SCC152 cells (Fig. 2E and F). As shown in Fig. 1F, the overexpression of CUL1 and UBE2L3 enhanced the ubiquitination of the HPV16 E7 protein. Thus, this may be due to the significantly increased CUL1 and UBE2L3 proteins by MG132, which enhance HPV16 E7 ubiquitination, compensating for proteasome inhibition. Additionally, the ubiquitinated forms of HPV16 E7 have higher molecular weights and slower electrophoretic mobility than the unmodified HPV16 E7, resulting in not being detected by western blotting.

Next, to assess if the HPV16 oncoproteins E6 and/or E7 are responsible for the low CUL1 and UBE2L3 protein levels, we measured CUL1 and UBE2L3 protein levels in N/Tert-1 cells expressing HPV16 E6 (N/Tert-1 E6), E7 (N/Tert-1 E7), and E6E7 (N/Tert-1 E6E7) compared to control N/Tert-1 cells containing an empty vector (N/Tert-1 vector) by western blotting. The E7 protein (Fig. 2G and H) and HPV16 E6 and E7 mRNA levels (Fig. 2I) in these N/Tert-1 cells were verified by western blotting and RT-qPCR, respectively. The results showed that the protein levels of both CUL1 and UBE2L3 were significantly decreased in HPV16 E6, HPV16 E7, and HPV16 E6E7 cells compared to N/Tert-1 vector cells (Fig. 2G and H). These results suggest that either E6 or E7 expression is sufficient for decreasing CUL1 and UBE2L3 protein levels in normal keratinocytes.

MARCHF8 knockdown increases the CUL1 and UBE2L3 protein levels and decreases the HPV16 E7 protein level in HPV+ HNC cells

The E3 ubiquitin ligase MARCHF8 ubiquitinates several cellular proteins for degradation. By analyzing proteomics data from a previous study in esophageal squamous cell

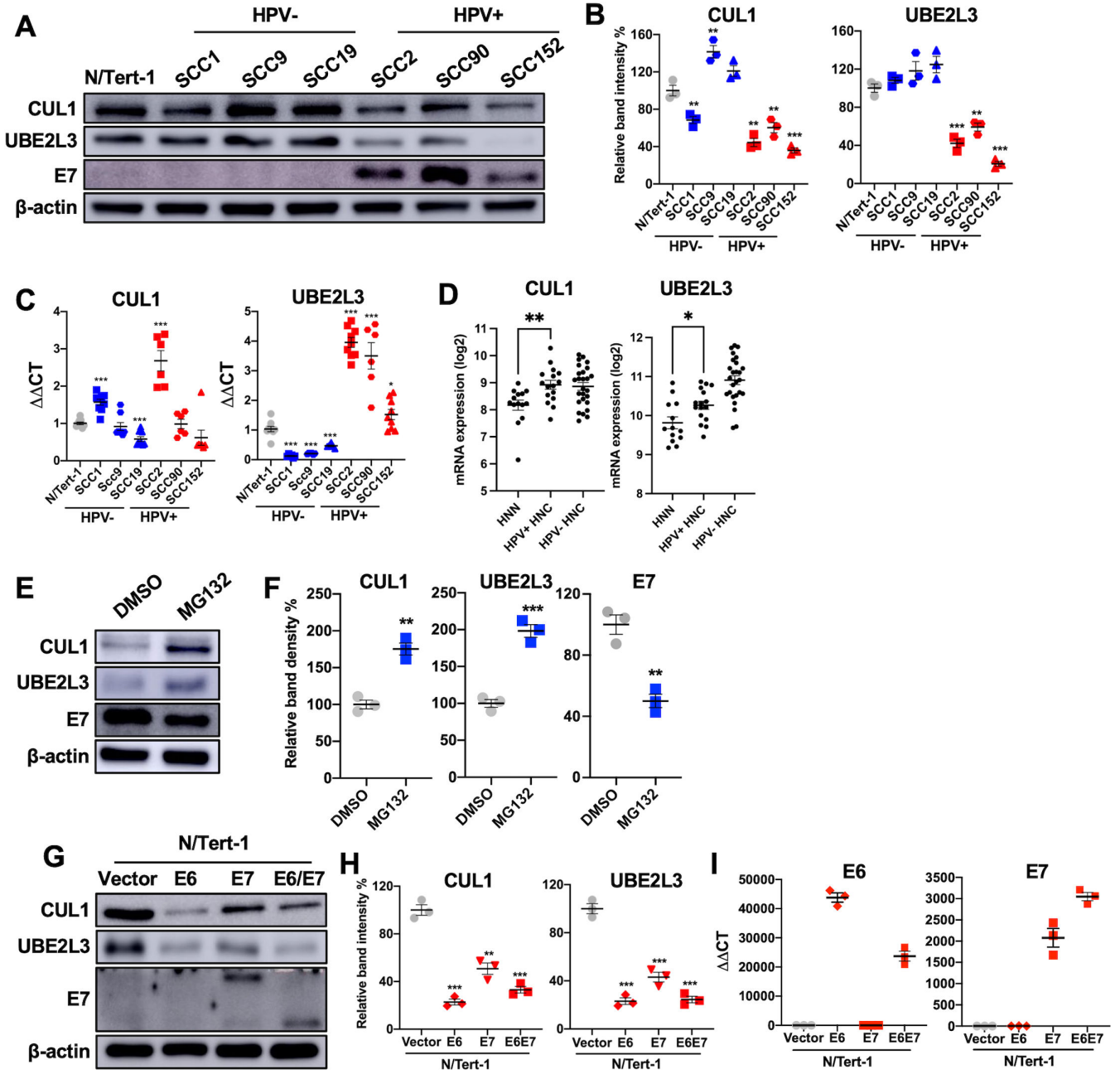

FIG 2 CUL1 and UBE2L3 protein levels are low in HPV+ HNC cells. CUL1 and UBE2L3 protein levels in normal (N/Tert-1), HPV- HNC (SCC1, SCC9, and SCC19), and HPV+ HNC (SCC2, SCC90, and SCC152) cells were determined by western blotting (A). Relative band intensities were quantified using NIH ImageJ (B). HPV16 E7 and β-actin were used as viral and internal controls, respectively. CUL1 and UBE2L3 mRNA expression levels in normal (N/Tert-1), HPV+ HNC (SCC2, SCC90, and SCC152), and HPV– HNC (SCC1, SCC9, and SCC19) cells were quantified by RT-qPCR (C). The data shown are normalized by the glyceraldehyde 3-phosphate dehydrogenase (GAPDH) mRNA level as an internal control. The mRNA expression levels of CUL1 and UBE2L3 were analyzed using our previous gene expression data (GSE6791) (2) and shown as fluorescence intensity (log2) from microdissected human tissue samples from HPV+ (n = 16) and HPV– (n = 26) HNC patients and normal individuals (n = 12) (D). CUL1, UBE2L3, and E7 protein levels in SCC152 cells treated with MG132 (10 μM) or dimethyl sulfoxide (DMSO) (E). Relative band intensities were quantified using NIH ImageJ (F). CUL1 and UBE2L3 proteins were detected in N/Tert-1 cells expressing HPV16 E6, E7, or E6 and E7 by western blotting (G). The size of HPV16 E7 in N/Tert-1 E7 cells is about 22 kDa due to HA tagging, while the size of native HPV16 E7 in N/Tert-1 E6E7 cells is about 17 kDa. Relative band intensities were quantified using NIH ImageJ (H). Total RNA was extracted from N/Tert-1 containing an empty vector and N/Tert-1 cells expressing HPV16 E6, E7, or E6 and E7 (E6E7). The HPV16 E6 and E7 mRNA levels were quantified by RT-qPCR (I). The data shown are normalized by the GAPDH mRNA level as an internal control. All experiments were repeated at least three times, and the data shown are means ± SD of three independent experiments. Student's t-test determined P-values. *P < 0.05, **P < 0.01, ***P < 0.001.

carcinoma (27), we found that the CUL1 and UBE2L3 proteins are among the cellular proteins increased by the MARCHF8 knockdown. Thus, we hypothesized that MARCHF8 plays an essential role in maintaining high HPV16 E7 protein levels in HPV+ HNC cells by degrading CUL1 and UBE2L3 proteins. To test the hypothesis, we knocked down MARCHF8 expression in two HPV+ HNC cells, SCC152 and SCC2, using multiple shRNAs against MARCHF8 (shR-MARCHF8) delivered by lentiviral transduction. All SCC152 (Fig. 3A and C) and SCC2 (Fig. 3B and D) cell lines with shR-MARCHF8 showed at least a 50% decrease in MARCHF8 protein levels compared to the cells with scrambled shRNA (shR-scr). As hypothesized, western blotting showed that CUL1 and UBE2L3 protein levels are significantly increased by MARCHF8 knockdown (Fig. 3A through D). Interestingly, HPV16 E7 protein levels are dramatically decreased by MARCHF8 knockdown, showing an inverse correlation with the CUL1 and UBE2L3 protein levels (Fig. 3A through D). The decreased HPV16 E7 protein levels are also validated by the significant increase in pRb protein levels by MARCHF8 knockdown (Fig. 3A through D). To test if MARCHF8 knockdown affects mRNA expression of CUL1 and UBE2L3, we measured mRNA levels of CUL1 and UBE2L3 in SCC152 and SCC2 cells with MARCHF8 knockdown by RT-qPCR. The results showed a significant decrease in CUL1 and UBE2L3 mRNA levels by MARCHF8 knockdown in SCC152 cells (Fig. 3E) but not in SCC2 cells (Fig. 3F). These results indicate that the increase of the CUL1 and UBE2L3 protein levels by MARCHF8 knockdown in HPV+ HNC cells is independent of CUL1 and UBE2L3 mRNA expression. We also observed a slight decrease in HPV16 E7 mRNA levels by MARCHF8 knockdown (Fig. 3E and F). However, as the E7 mRNA levels are still high despite the MARCHF8 knockdown, it is unlikely that the slight decrease of E7 mRNA levels entirely causes the considerable reduction of the HPV16 E7 protein levels by the MARCHF8 knockdown. Thus, our findings suggest that HPV-induced MARCHF8 is responsible for the low CUL1 and UBE2L3 and high HPV16 E7 protein levels in HPV+ HNC cells.

MARCHF8 interacts with and ubiquitinates CUL1 and UBE2L3 proteins in HPV+ HNC cells

As MARCHF8 knockdown increased CUL1 and UBE2L3 protein levels (Fig. 3A and B), we hypothesized that HPV-induced MARCHF8 ubiquitinates CUL1 and UBE2L3 proteins for proteasomal degradation. First, to determine if MARCHF8 binds to CUL1 and UBE2L3, we pulled down MARCHF8 protein in whole cell lysates from SCC152 cells treated with MG132 using anti-MARCHF8 antibody-conjugated magnetic beads. We detected CUL1 and UBE2L3 proteins by western blotting. The results showed that CUL1 and UBE2L3 proteins were co-immunoprecipitated with MARCHF8 protein (Fig. 4A). In contrast, HPV16 E7 protein was not co-immunoprecipitated with MARCHF8 protein (Fig. 4A), indicating that HPV16 E7 may not be a direct target of MARCHF8. Reciprocally, we pulled down CUL1 or UBE2L3 proteins in the same whole cell lysates from MG132-treated SCC152 cells using anti-CUL1 or anti-UBE2L3 antibodies, respectively and found that MARCHF8 protein is co-immunoprecipitated with CUL1 and UBE2L3 proteins (Fig. 4B and C). These results suggest that the MARCHF8 protein interacts with CUL1 and UBE2L3 but not the HPV16 E7 protein.

Next, to determine if MARCHF8 ubiquitinates CUL1 and UBE2L3 proteins, we pulled down ubiquitinated proteins in whole cell lysates from MG132-treated SCC152 cells using anti-ubiquitin antibody-conjugated magnetic beads. The results showed that ubiquitinated forms of CUL1 (Fig. 4D) and UBE2L3 (Fig. 4E) proteins were decreased in SCC152 cells with MARCHF8 knockdown despite the significantly higher levels of total input CUL1 and UBE2L3 proteins compared to SCC152 cells with shR-scr (Fig. 4D and E). These results suggest that the decrease of CUL1 and UBE2L3 protein levels in HPV+ HNC cells is likely mediated by MARCHF8-driven ubiquitination and protein degradation. To determine if the ubiquitination of HPV16 E7 protein is increased by MARCHF8 knockdown, we detected HPV16 E7 protein from the same pulldowns of ubiquitinated proteins. We found that the levels of ubiquitinated HPV16 E7 protein were dramatically increased by MARCHF8 knockdown, showing an inverse correlation with the

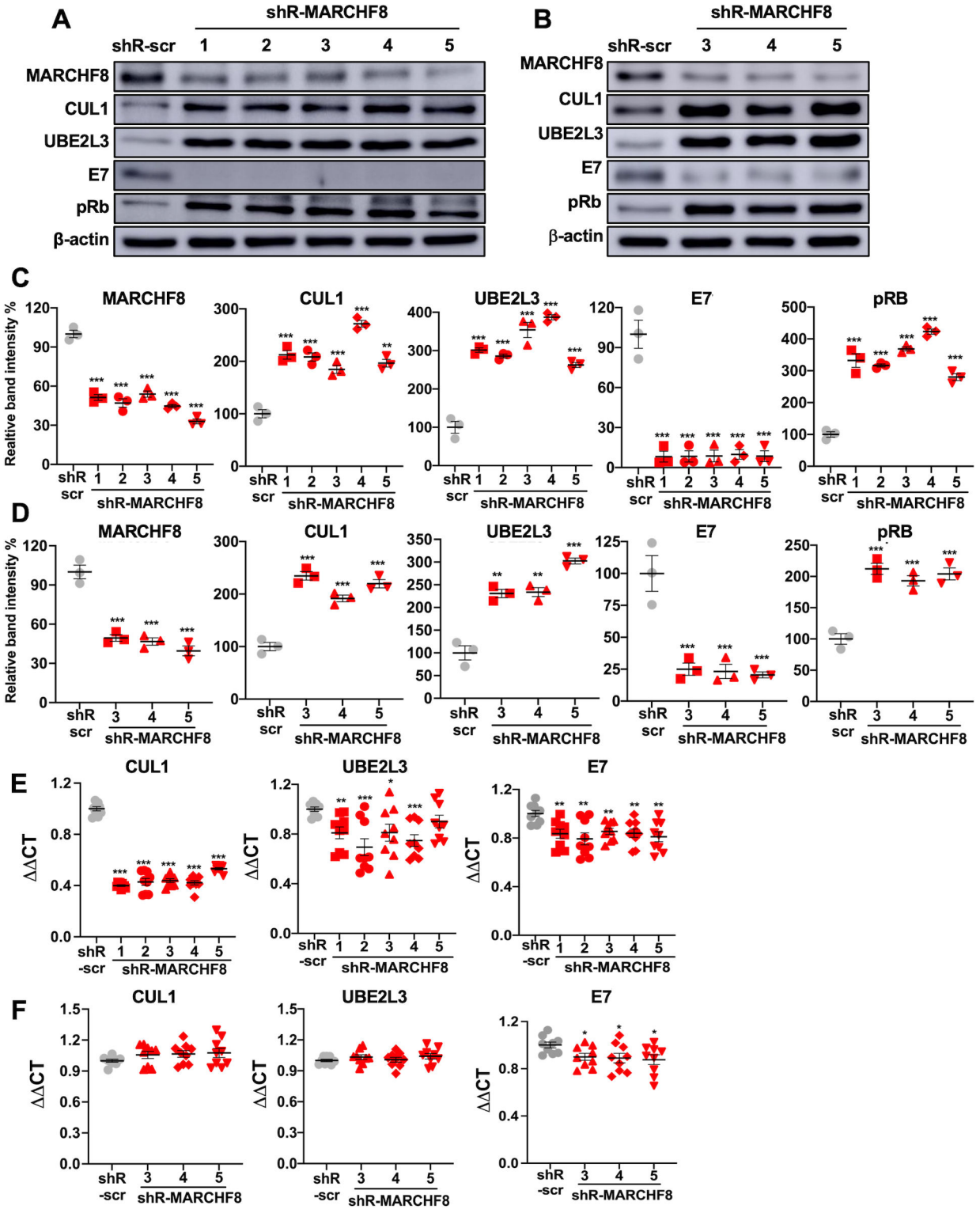

FIG 3 Knockdown of MARCHF8 expression increases CUL1 and UBE2L3 protein levels and decreases HPV16 E7 protein levels in HPV+ HNC cells. SCC152 (A and C) and SCC2 (B and D) cells were transduced with five and three lentiviral shR-MARCHF8, respectively, or shR-scr as a control. MARCHF8, CUL1, UBE2L3, HPV16 E7, and pRb proteins in SCC152 (A) and SCC2 (B) cells were detected by western blotting. The relative band intensities were quantified using NIH ImageJ (C and D). β-Actin was used as an internal control. The mRNA levels of CUL1, UBE2L3, and HPV16 E7 were quantified by RT-qPCR in SCC152 (E) and SCC2 (F) cells transduced with five and three lentiviral shR-MARCHF8, respectively, or shR-scr as a control. The data shown are normalized by the GAPDH mRNA level as an internal control. The data shown are means ± SD of three independent experiments. Student's *t*-test determined *P*-values. **P* < 0.05, ***P* < 0.01, ****P* < 0.001.

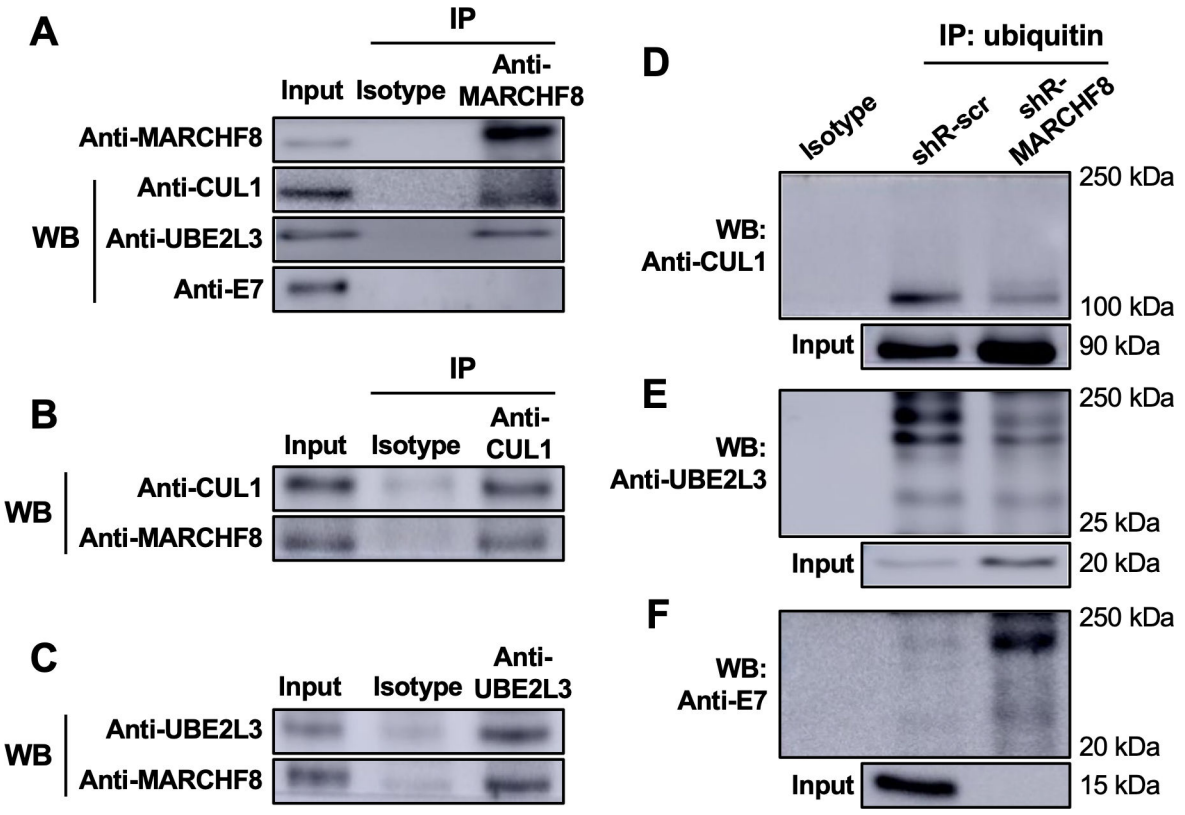

FIG 4 MARCHF8 protein interacts with and ubiquitinates CUL1 and UBE2L3 proteins. MARCHF8 (A), CUL1 (B), and UBE2L3 (C) were pulled down from the lysate of SCC-152 cells treated with MG132 (10 µM) using anti-MARCHF8 (A), anti-CUL1 (B), and anti-UBE2L3 (C) antibodies, respectively. CUL1, UBE2L3, HPV16 E7, and MARCHF8 were detected from the immunoprecipitated proteins by western blotting. (D–F) Ubiquitinated proteins were pulled down from the lysate of SCC152 cells with shR-scr or shRNA against MARCHF8 (shR-MARCHF8 clone 3) treated with MG132 (10 µM) using anti-ubiquitin antibody-conjugated magnetic beads. CUL1 (D), UBE2L3 (E), and HPV16 E7 (F) proteins were detected in the immunoprecipitated proteins by western blotting. All experiments were repeated at least three times. The data shown are means ± SD of three independent experiments. Student's *t*-test determined *P*-values. $^{*}P < 0.05$, $^{**}P < 0.01$, $^{***}P < 0.001$.

ubiquitination levels of CUL1 and UBE2L3 proteins (Fig. 4F). Together, these results suggest that MARCHF8 binds to and ubiquitinates CUL1 and UBE2L3 to prevent ubiquitination of HPV16 E7.

MARCHF8 knockdown suppresses HPV+ HNC cell proliferation

It is well known that the oncoprotein E7 promotes cell cycle progression and proliferation of HPV-infected cells (32, 33). Thus, we tested if the decrease of HPV16 E7 protein levels by MARCHF8 knockdown inhibits the proliferation of SCC152 and SCC2 cells by counting cell numbers over time. The results showed that MARCHF8 knockdown significantly decreases the cell numbers of SCC152 (Fig. 5A) and SCC2 (Fig. 5B) cells compared to the corresponding control cells with shR-scr. In addition, to determine if MARCHF8 knockdown inhibits the cell cycle progression of HPV+ HNC cells, we stained SCC152 and SCC2 cells with bromodeoxyuridine (BrdU) and the Zombie NIR for measuring *de novo* DNA synthesis and cell viability, respectively, and analyzed labeled cells by flow cytometry. The results showed that BrdU incorporation in SCC152 and SCC2 cells is significantly decreased by MARCHF8 knockdown (Fig. 5C and D). These results suggest that MARCHF8 knockdown decreases the proliferation of HPV+ HNC cells, likely due to the reduction of HPV16 E7 protein levels.

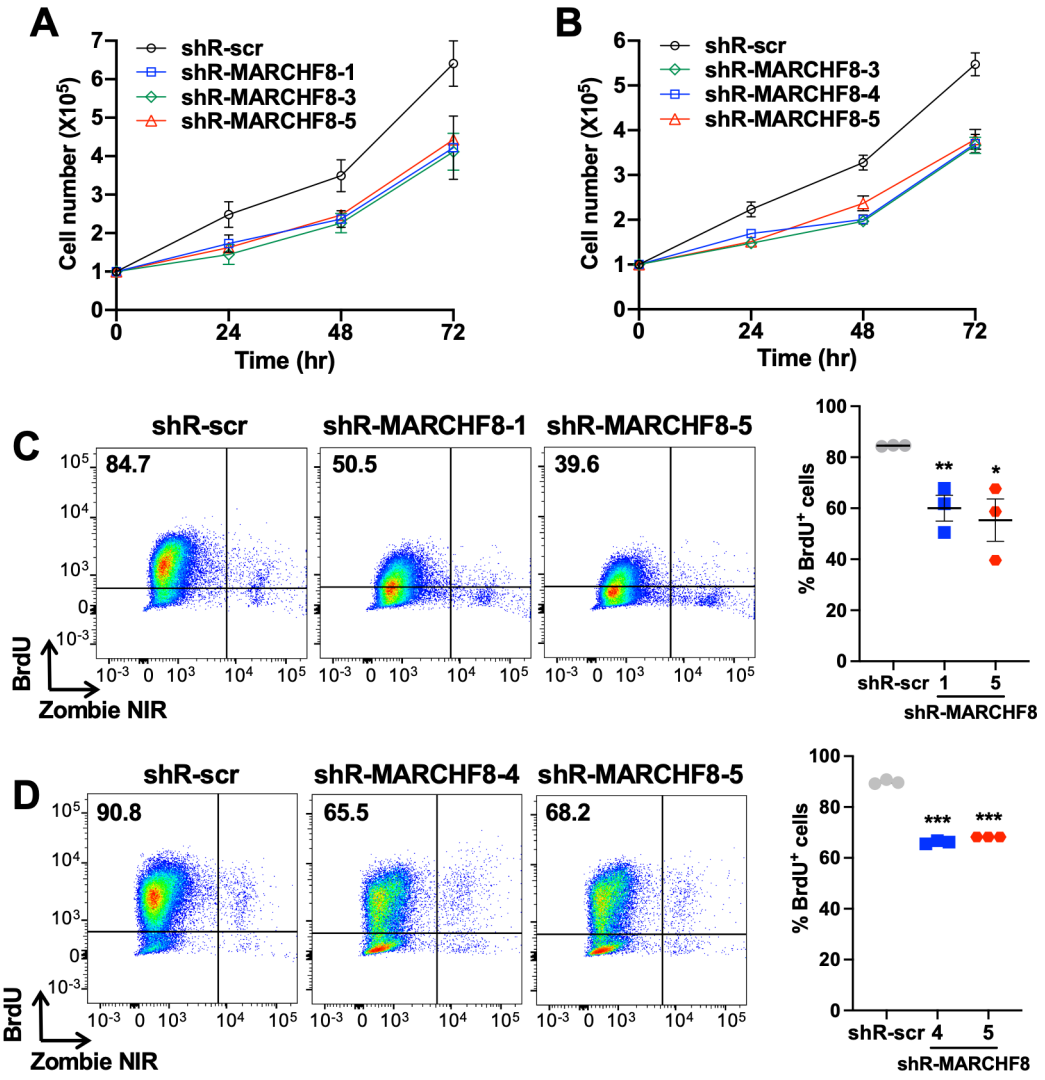

FIG 5 Knockdown of MARCHF8 expression suppresses proliferation of HPV+ HNC cells. Cell proliferation rate was determined by cell counting using two HPV+ HNC cell lines, SCC152 (A) and SCC2 (B), with shR-scr or three shR-MARCHF8. 1×10^5 cells per well were seeded in a six-well plate. The cells were detached and counted at 24, 48, and 72 hours. BrdU incorporation assays were performed with SCC152 (shR-MARCHF8 clones 1 and 5) (C) and SCC2 (shR-MARCHF8 clones 4 and 5) (D) cells with MARCHF8 knockdown. 1×10^6 cells were seeded in 10 cm Petri dishes and incubated for 16 hours with BrdU (10 mM). BrdU incorporation was analyzed by flow cytometry. Cell viability was determined by Zombie NIR staining as a control. All experiments were repeated at least three times, and the data shown are means ± SD. Student's *t*-test determined *P*-values. ***$P < 0.001$.

Marchf8 knockout in HPV+ mouse oral cancer cells restores CUL1 and UBE2L3 protein levels and decreases HPV16 E7 protein levels

To investigate if the degradation of HPV16 E7 protein by CUL1 and UBE2L3 inhibits tumor growth, we utilized a C57BL/6J (B6) mouse oral epithelial (MOE) cell line expressing HPV16 E6/E7 and *Hras* (mEERL) which forms tumors in immunocompetent syngeneic B6 mice (34). First, the protein levels of MARCHF8, CUL1, and UBE2L3 in mEERL cells were determined by comparing them to normal immortalized MOE cells (NiMOE) and mouse HPV– MOE cells transformed with *Hras* and shR-Ptpn14 (MOE/shPtpn14). Consistent with those from human HNC cells, the results showed significantly higher MARCHF8 and lower CUL1 and UBE2L3 protein levels in mEERL cells compared to NiMOE cells and HPV– MOE cells (Fig. 6A and B). These results suggest that mEERL cells recapitulate our findings from

human HPV+ HNC cells, showing that HPV-induced MARCHF8 degrades the CUL1 and UBE2L3 proteins. Although there is a significant increase in MARCHF8 protein in HPV− MOE compared to NiMOE cells, the CUL1 and UBE2L3 protein levels are not reduced (Fig. 6A and B). This result suggests that MARCHF8 requires an additional factor(s), expressed in HPV+ HNC cells but not in HPV− HNC cells, for CUL1 and UBE2L3 ubiquitination and degradation.

Next, to determine if high MARCHF8 protein levels in mEERL cells are responsible for the low CUL1 and UBE2L3 protein levels, we measured CUL1 and UBE2L3 protein levels in *Marchf8* knockout mEERL cell lines (mEERL/*Marchf8*$^{-/-}$) previously established using CRISPR/Cas9 (31). Western blotting confirmed that mEERL/*Marchf8*$^{-/-}$ cells have significantly increased CUL1 and UBE2L3 protein levels and decreased HPV16 E7 protein levels compared to mEERL cells with the scrambled control sgRNA (mEERL/scr) (Fig. 6C and D). These results are consistent with human HPV+ HNC cells presented in Fig. 3, suggesting that HPV-induced increase of MARCHF8 in HPV+ HNC cells stabilizes HPV16 E7 protein by degrading CUL1 and UBE2L3.

Cul1 and *Ube2l3* overexpression in HPV+ mouse oral cancer cells delays tumor growth *in vivo*

To determine whether *Cul1 and Ube2l3* overexpression suppresses HPV+ HNC tumor growth, we generated mEERL cells overexpressing *Cul1* (mEERL/*Cul1*) or *Ube2l3* (mEERL/*Ube2l3*) using lentiviruses and blasticidin selection. Consistent with the results from human HPV+ HNC cells (Fig. 1B through E), *Cul1* or *Ube2l3* overexpression decreased the HPV16 E7 protein level in mEERL cells (Fig. 7A and B). Next, ten C57BL/6J mice were subcutaneously injected with 5×10^5 of either mEERL/*Cul1,* mEERL/*Ube2l3,* or mEERL/scr cells. The results show that all 10 mice injected with mEERL/vector cells vigorously grew tumors (Fig. 7C and F) and succumbed to tumor burden within ~7 weeks post-injection (Fig. 7G). In contrast, the mice injected with mEERL/*Cul1 or* mEERL/*Ube2l3* cells displayed delayed tumor formation and death by tumor burden (Fig. 7D and G). Our results suggest that *Cul1* or *Ube2l3* overexpression results in HPV16 E7 protein degradation and tumor suppression.

DISCUSSION

The HPV oncoprotein E7 is essential for virus replication (35), and its continuous expression at high levels is required for HPV-associated cancer progression and maintenance (5, 6, 36, 37). HPV16 E7 interacts with several E3 ubiquitin ligases to facilitate carcinogenesis. It is well understood that E7 induces the proteasomal degradation of various tumor suppressors, such as pRb and mediator of cell motility 1, by interacting with the CUL2 ubiquitin ligase complex (13, 16, 38, 39). In contrast, E7 also stabilizes host proteins such as the apolipoprotein B mRNA editing enzyme catalytic polypeptide-like 3 (APOBEC3A), a hypoxia-inducible factor (HIF-1a), p53, and p21 (12, 40–42). The dual functions of E7 in host protein degradation suggest intertwined interactions between E7 and various ubiquitin ligases in host cells.

Despite its essential role in cancer progression and maintenance, the E7 protein can be efficiently ubiquitinated and degraded by host factors. E7 protein has a relatively short half-life of less than 1 hour (43, 44). Mechanistically, the SCF (Skp-Cullin-F box) ubiquitin ligase complex containing CUL1 and UBE2L3 mediates E7 ubiquitination and degradation (17). Although HPV16 E7 contains two lysine residues in positions 60 and 97 (44), the 11 amino acids at the N-terminal residues are essential for ubiquitination and degradation (44). Substituting the two lysines K60 and K97 to arginine in the E7 protein did not abrogate its ubiquitination. In contrast, deleting the N-terminal 11 amino acids prevented E7 ubiquitination and stabilized HPV16 E7 proteins (44). Mechanistically, the free N-terminal residue of E7 is first linearly ubiquitinated, and then other ubiquitin groups are attached to the internal lysine of the first ubiquitin moiety at the N-terminal residue (44). The lysine-independent ubiquitination of E7 proteins is similar to the

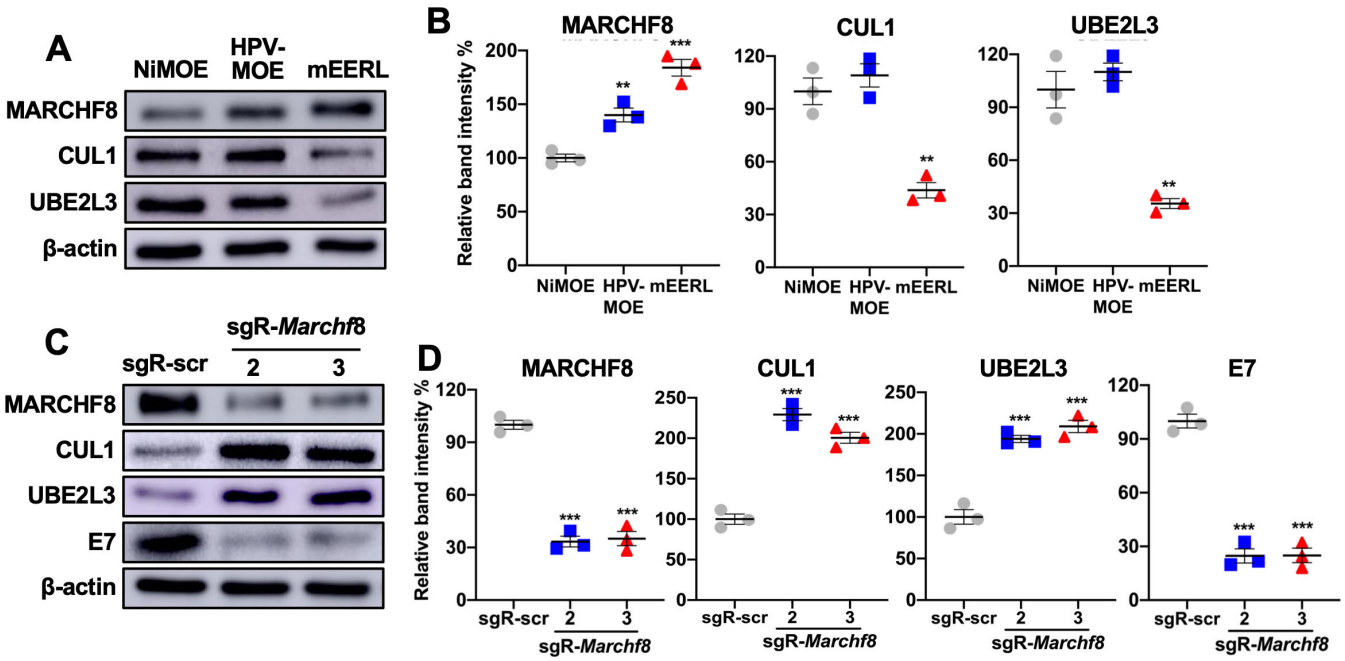

FIG 6 *Marchf8* knockout restores CUL1 and UBE2L3 protein levels in HPV+ mouse oral cancer cells. CUL1 and UBE2L3 protein levels in mouse normal immortalized (NiMOE), HPV− transformed (HPV− MOE), and HPV+ transformed (mEERL) oral epithelial cells were determined by western blotting (A). β-actin was used as an internal control. The relative band intensities were quantified using NIH ImageJ (B). mEERL cells were transduced with lentiviruses containing Cas9 and one of two sgRNAs against Marchf8 (sgR-*Marchf*8-2 and sgR-*Marchf*8-3) or scrambled sgRNA (sgR-scr). MARCHF8, CUL1, UBE2L3, and HPV16 E7 proteins were detected by western blotting (C). Relative band intensities were quantified using NIH ImageJ (D). The data shown are means ± SD of three independent experiments. All experiments were repeated at least three times, and the data shown are means ± SD. Student's *t*-test determined *P*-values. **P* < 0.05, ****P* < 0.001.

mechanism by which MyoD (45) and Epstein Barr virus latent membrane protein 1 (46) is ubiquitinated (44).

To maintain the high E7 levels in HPV+ cancer cells, E7 proteins are stabilized through several mechanisms, such as deubiquitination and phosphorylation (25, 26). First, E7 binds to several ubiquitin-specific proteases (USPs) that remove ubiquitin from ubiquitinated proteins (47). Previous studies have shown that USP7 and USP11 deubiquitinate and stabilize E7 proteins (25, 48). In addition, dual-specificity tyrosine phosphorylation-regulated kinase 1A phosphorylates HPV16 E7 and prolongs the E7 protein half-life by hindering ubiquitinated E7 binding to proteasomes (26). E7 proteins are also stabilized by an E6^E7 fusion protein from an E6^E7 splice isoform that encodes 41 N-terminal amino acids of E6 and 38 C-terminal amino acids of E7 (49). The E6^E7 fusion protein binds to and stabilizes both E6 and E7 proteins in the presence of GRP78 and HSP90 (49). A recent study has also shown that E6AP overexpression stabilizes E7 protein in a proteasome-dependent manner (50). While these previous reports suggest that E7 protein can be stabilized through various mechanisms, it is still unknown how E7 protein overcomes its degradation mediated by the SCF ubiquitin ligase complex containing CUL1 and UBE2L3. Our findings reveal a novel mechanism of E7 protein stabilization by degrading CUL1 and UBE2L3, the important components of the SCF ubiquitin ligase complex.

The SCF ubiquitin ligase complex is characterized by a substrate recognition factor for connecting the substrate to the E3 ubiquitin ligase complex. The adaptor is a limiting factor for the targeted process and substrates. The SCF ubiquitin ligase complex has a central role in cell cycle regulation. Deregulated cell cycle control is a hallmark of cancer. The F box protein adaptor targets negative cell cycle regulators, such as cyclins (A, D, and E) (51), p21 (18), p27 (19), and p57 (52), for ubiquitination and degradation (53). Hence, it promotes cell cycle progression during S and G2 phases (53). Several studies have shown

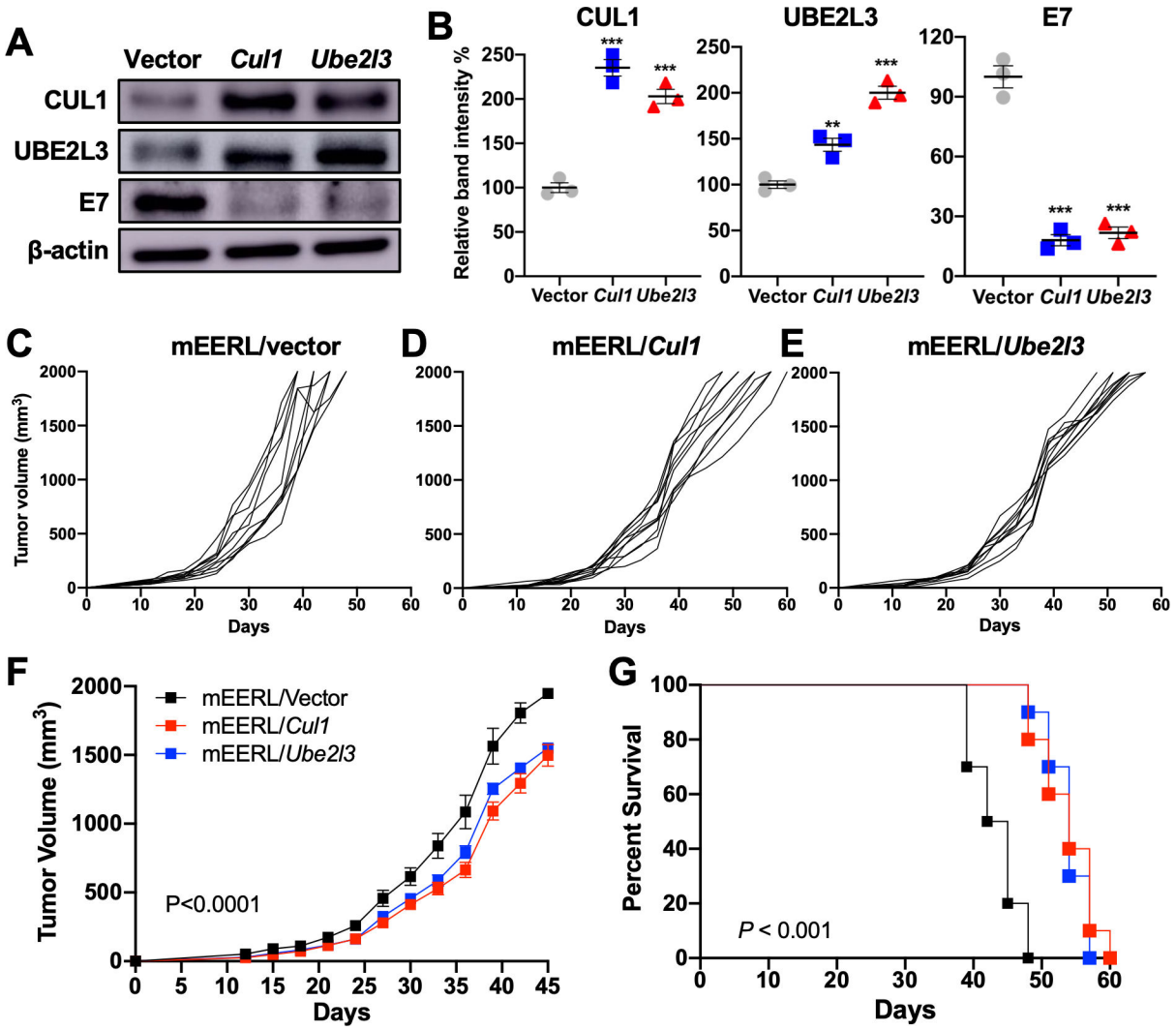

FIG 7 CUL1 and UBE2L3 overexpression suppresses HPV+ HNC tumor growth *in vivo*. mEERL cells overexpressing *Cul1* or *Ube2l3* were generated by lentiviral transduction of the *Cul1* or *Ube2l3* genes, respectively, and blasticidin selection. CUL1, UBE2L3, and HPV16 E7 proteins were detected by western blotting (A). Relative band intensities were quantified using NIH ImageJ (B). β-actin was used as an internal control. The data shown are means ± SD of three independent experiments. Student's *t*-test determined *P*-values. **P* < 0.05, ***P* < 0.01, ****P* < 0.001. mEERL/vector (C), mEERL/*Cul1* (D), or mEERL/*Ube2l3* (E) cells were injected into the rear right flank of C57BL/6J mice (*n* = 10 per group). Tumor volume was measured twice a week (C–F). Survival rates of mice were analyzed using a Kaplan-Meier estimator (G). The time to event was determined for each group, with the event defined as a tumor size larger than 2,000 mm^3. The data shown are means ± SD. *P*-values of mice injected with mEERL/*Cul1 and* mEERL/*Ube2l3* cells compared with mice injected with mEERL/vector cells were determined for tumor growth (F) and survival (G) by two-way analysis of variance. Shown are representative of two independent experiments.

that CUL1 is upregulated in many cancers and is associated with poor patient prognosis in various cancers, including gastric, breast, renal cell carcinoma, colorectal, and hepatocellular carcinoma (54–58). Additionally, CUL1 augments cancer cell proliferation, adhesion, migration, and metastasis (54–59). On the other hand, the SCF ubiquitin ligase complex binds to RNA-binding proteins of the fragile X protein family FMRP, FXR1, and FXR2 in HPV-negative HNC cells (60). The SCF ubiquitin ligase complex binding to these RNA-binding proteins led to their degradation and suppressed tumorigenesis (60). Additionally, our results show that CUL1 overexpression in HPV+ HNC cells hinders cell proliferation and delays tumor growth *in vivo*.

Ubiquitination and degradation of p53 by E6 and E6AP are hallmarks of HPV-associated cancer progression. UBE2L3, an E2 conjugating enzyme, is essential in the E6AP E3 ubiquitin ligase complex for ubiquitinating p53 (61). However, UBE2L3 upregulation

by AhR activation in HeLa cells inhibits cell proliferation and enhances apoptosis (62, 63). This result may be caused by E7 degradation as UBE2L3 and CUL1 ubiquitinate and degrade E7 proteins in cervical cancer cells (17). In contrast, UBE2L3, associated with the SCF ubiquitin ligase complex, promotes non-small cell lung cancer by ubiquitinating and degrading p27kip1 and glycogen synthase kinase 3β (GSK-3β) (64, 65). Thus, CUL1 and UBE2L3 might have double-edged functions for tumor promotion in lung cancer while suppressing HPV+ cancers through E7 degradation.

We report here that MARCHF8 plays a vital role in HPV16 E7 protein stabilization in HPV+ HNC cells by degrading CUL1 and UBE2L3 (Fig. 8). As E7 is required for viral replication, this finding suggests that MARCHF8 contributes to HPV infection and persistence. Likewise, recent studies have shown that MARCHF8 supports infection of several human viruses, including HCV, dengue, and Zika (66). Particularly, MARCHF8 induces the polyubiquitination of the HCV nonstructural2 protein that mediates binding to ESCRT0 and assembling viral envelope (67, 68). Additionally, MARCHF8 facilitates HIV infection by ubiquitinating and degrading tetherin independent of Vpu (69). In contrast, MARCHF8 is also known as an antiviral restriction factor (66). MARCHF8 targets several viral envelope glycoproteins to inhibit infections of HIV, vesicular stomatitis virus, rabies virus, lymphocytic choriomeningitis virus, severe acute respiratory syndrome coronavirus (SARS-CoV), chikungunya virus, and Ross River virus (70–72). Moreover, MARCHF8 also restricts influenza A virus infectivity by inhibiting the incorporation of the virus glycoproteins into the progeny virions (73) and targeting the M2 protein for ubiquitin-dependent degradation (74). These findings suggest that MARCHF8 plays a dual role in virus infection as a proviral and antiviral factor.

As E7 is required for HPV replication and carcinogenesis, destabilizing E7 proteins by targeting MARCHF8 may effectively prevent and treat HPV-associated cancers. Additionally, we have recently shown that MARCHF8 ubiquitinates and degrades death receptors to impede apoptosis of HPV+ HNC cells and that *MARCHF8* knockout significantly suppresses tumor growth *in vivo* (31). Taken together, our findings suggest MARCHF8 as a potential therapeutic target for HPV+ HNC. Figure generated using Biorender icons.

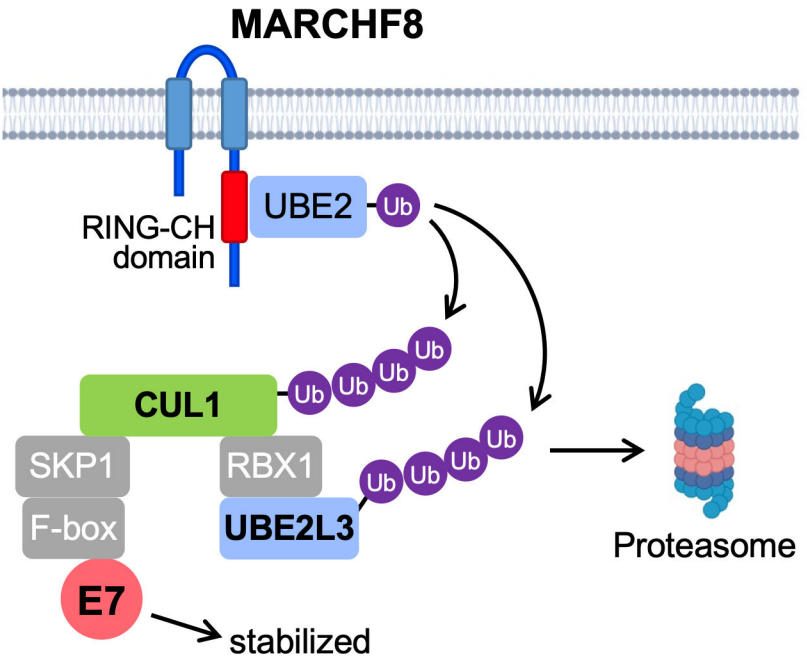

FIG 8 The schematic model of MARCHF8-mediated HPV16 E7 stabilization by degrading CUL1 and UBE2L3. The HPV16 oncoprotein E6 activates the *MARCHF8* promoter activity through the MYC/MAX transcription factor complex and upregulates MARCHF8 in the HPV+ HNC cells (31). MARCHF8 protein ubiquitinates and degrades CUL1 and UBE2L3 proteins, leading to the prevention of HPV16 E7 protein degradation.

MATERIALS AND METHODS

Cell lines

293FT cells were obtained from Thermo Fisher (Waltham, MA). HPV+ HNC (SCC2, SCC90, and SCC152) and HPV− HNC (SCC1, SCC9, and SCC19) cells were purchased from the American Type Culture Collection (Manassas, VA). These cells were maintained in Dulbecco's Modified Eagle's Medium (DMEM) containing 10% fetal bovine serum (FBS) and penicillin/streptomycin (Thermo Fisher) as described (12, 75–77). The N/Tert-1 cell (78) expressing HPV16 E6 (N/Tert-1-E6), E7 (N/Tert-1-E7), and E6 and E7 (N/Tert-1-E6E7) were previously established (79, 80) and cultured in keratinocyte serum-free medium containing epidermal growth factor (EGF), bovine pituitary extract, and penicillin/streptomycin (Thermo Fisher). The MOE cell lines, NiMOE, mEERL (HPV+), and MOE/shPtpn13 (HPV−), were obtained from John Lee (34) and maintained in E-medium (DMEM and F12 media containing 0.005% hydrocortisone, 0.05% transferrin, 0.05% insulin, 0.0014% triiodothyronine, 0.005% EGF, and 2% FBS) as previously described (81).

Lentivirus constructs and production

The human *CUL1* and *UBE2L3* coding sequences were amplified from pcDNA-HA-UBE2L3 (Addgene, #27561) and pcDNA-myc3-CUL1 (Addgene, #19896), respectively, and cloned into the pLenti6/V5-D-TOPO backbone (Addgene, #22945). The mouse *Cul1* and *Ube2l3* coding sequences were amplified from cDNA prepared from NiMOE cells and cloned into the pLenti6/V5-D-TOPO backbone (Addgene, #22945). The primer sequences used in amplifying human and mouse *CUL1* and *UBE2L3* coding sequences are listed in Table 1. The shRNAs targeting human *MARCHF8* were ordered from Sigma-Aldrich (St. Louis, MO). The sgRNAs targeting *Marchf8* were designed using the web-based software ChopChop (chopchop.cbu.uib.no) (82) and cloned into the lentiCRISPR v2-blast plasmid (Addgene, #83480) using ligating duplex oligonucleotides containing BsmBI restriction sites purchased from Integrated DNA Technologies (IDT, Coralville, IA). The shRNAs and sgRNAs used are listed in Tables 2 and 3. Lentiviruses containing human and mouse *CUL1*, *UBE2L3*, and shRNA or sgRNA against MARCHF8 were produced using 293FT cells with packaging constructs, pCMV-VSV-G (Addgene, #8454) and pCMV-Delta R8.2 (Addgene, #12263). The lentiviruses were harvested 48 hours post-transfection and concentrated by ultracentrifugation at 25,000 rpm for 2 hours. In addition, cells were incubated with lentiviruses for 48 hours in the presence of polybrene (8 µg/mL) and selected with blasticidin (8 µg/mL).

TABLE 1 List of the oligonucleotides[a]

Name	Sequence	Experiment
Human GAPDH Fwd	5′-GGAGCGAGATCCCTCCAAAAT-3′	RT-qPCR
Human GAPDH Rev	5′-GGCTGTTGTCATACTTCTCATGG-3′	RT-qPCR
Human UBE2L3 Fwd	5′-CAACTTTCCAGCAGAGTACCC-3′	RT-qPCR
Human UBE2L3 Rev	5′-TGCCCCTTTTCGTCGATGTTT-3′	RT-qPCR
Human Cullin1 Fwd	5′-AGCCATTGAAAAGTGTGGAGAA-3′	RT-qPCR
Human Cullin1 Rev	5′-GCGTCATTGTTGAATGCAGACA-3′	RT-qPCR
HPV16 E7 Fwd	5′-GTGACAGCTCAGAGGAGGAGGATG-3′	RT-qPCR
HPV16 E7 Rev	5′-ACGCACAACCGAAGCGTAGAGTCA-3′	RT-qPCR
Human UBE2L3 Fwd	5′-CACGTGGGATCCATGGATATCTATCCAT-3′	Cloning
Human UBE2L3 Rev	5′-CACGTGACCGGTTTAGTCCACAGGTCGC-3′	Cloning
Human Cullin1 Fwd	5′-CACGTGGGATCCATGGAATTCAGGATCCCCATG-3′	Cloning
Human Cullin1 Rev	5′-CACGTGACCGGTTTAAGCCAAGTAACTG-3′	Cloning
Mouse *Ube2l3* Fwd	5′-TCTAGAGGATCCAATGGCGGCCAGCAGG-3′	Cloning
Mouse *Ube2l3* Rev	5′-TTACTAACCGGTACGTTAGTCCACAGG-3′	Cloning
Mouse *Cullin1* Fwd	5′-TCTAGAGGATCCAATGTCATCAAACAGG-3′	Cloning
Mouse *Cullin1* Rev	5′-TACTAACCGGTACGTTAAGCCAAGTAAC-3′	Cloning

[a]Fwd, forward primer; GAPDH, glyceraldehyde 3-phosphate dehydrogenase; Rev, reverse primer.

TABLE 2 List of the shRNAs

Name	Sigma-Aldrich TRC clone ID	Sequence
Human MARCHF8 shRNA1	TRCN0000073233	5′-CTTGAGCTGAATGAGAGAATA-3′
Human MARCHF8 shRNA2	TRCN0000073234	5′-CCACTAACAGAGCCCAACTTT-3′
Human MARCHF8 shRNA3	TRCN0000073235	5′-CAGTGTAAAGTGTATGTGCAA-3′
Human MARCHF8 shRNA4	TRCN0000073236	5′-CTGGTCCTTGTATGTGCTCAT-3′
Human MARCHF8 shRNA5	TRCN0000073237	5′-CCTCCTTCTCTCGCACTTCTA-3′

BrdU staining

1×10^6 SCC152 and SCC2 MARCHF8 knockdown and scrambled cells were seeded per 10 cm^2 Petri dish in DMEM supplemented with 10% FBS and penicillin/streptomycin. Cells were incubated with a medium containing 10 mM BrdU for 16 hours. Cells were trypsinized and stained using a BrdU staining kit (Thermo Fisher) according to the manufacturer's instructions. Cell viability was determined by staining cells using the Zombie NIR kit (BioLegend). Stained cells were analyzed using an LSRII flow cytometer.

Immunoprecipitation (IP) and western blotting

Whole-cell lysates were prepared in 1× radioimmunoprecipitation assay buffer (Abcam, Waltham, MA) containing protease inhibitor cocktail (Roche, Mannheim, Germany) according to the manufacturer's instructions. The protein concentration was measured by the Pierce BCA Protein Assay Kit (Thermo Fisher). IP was performed using the Pierce Classic Magnetic IP/Co-IP Kit (Thermo Fisher). Briefly, 25 µL of protein A/G magnetic beads were incubated with 5 µg of specific antibodies (Table 4) for 2 hours. One to two milligrams of the whole cell lysates were incubated with antibody-coupled beads overnight at 4°C. In addition, 10 µg–20 µg of protein was used to perform western blotting with antibodies listed in Table 4 as previously described (83). NIH ImageJ software was used to determine band intensities and normalized to the β-actin band intensity.

RT-qPCR

RNeasy Plus Mini Kit (Qiagen, Germantown, MD) was used to extract total RNA. First-strand cDNA was synthesized from 2 µg of total RNA using Superscript II reverse transcriptase (Roche, Mannheim, Germany). qPCR was performed in a 20 µL reaction mixture containing 10 µL of SYBR Green Master Mix (Applied Biosystems), 5 µL of 1 mM primers, and 100 ng of cDNA template using a Bio-Rad CFT Connect thermocycler. Data were normalized to glyceraldehyde 3-phosphate dehydrogenase. IDT synthesized primers used in qPCR can be found in Table 1.

Mice and tumor growth

C57BL/6J mice were purchased from Jackson Laboratory (Bar Harbor, ME) and maintained by the USDA guidelines. 5×10^5 mEERL cells were subcutaneously injected

TABLE 3 List of the sgRNAs[a,b]

Name	Sequence
Mouse *Marchf8* sgRNA1 Fwd	5′-CACCG**AGGTGAGTATATGGGCCGTGAGG**-3′
Mouse *Marchf8* sgRNA1 Rev	5′-AAAC**CCTCACGGCCCATATACTCACCT**-3′
Mouse *Marchf8* sgRNA2 Fwd	5′-CACCG**TATTAACGTCTGACCATGTGAGG**-3′
Mouse *Marchf8* sgRNA2 Rev	5′-AAAC**CCTCACATGGTCAGACGTTAATA**-3′
Mouse *Marchf8* sgRNA3 Fwd	5′-CACCG**ACTACCAGCTTCGTCCAGAAAGG**-3′
Mouse *Marchf8* sgRNA3 Rev	5′-AAAC**CCTTTCTGGACGAAGCTGGTAGT**-3′

[a]Fwd, forward oligo; Rev, reverse oligo.
[b]The bolded letters indicate the sgRNA sequence, while the unbolded letters indicate the overhang sequence.

TABLE 4 List of the antibodies

Antibody	Specificity	Source	Catalog	RRID	Experiment
E7 (clone ED17)	HPV16	Santa Cruz	SC-6981	AB_627745	Western blot
MARCHF8	Human/Mouse	Thermo Fisher	PA5-88893	AB_2805201	Western blot
MARCHF8	Human/Mouse	Proteintech	14119–1-AP	AB_2140168	IP
Ubiquitin	Human/Mouse	Proteintech	10201–2-AP	AB_671515	IP-WB
UBE2L3	Human/Mouse	Proteintech	14115–1-AP	AB_2210891	IP-WB
Cullin1	Human/Mouse	Thermo Fisher	71–8700	AB_2534002	IP-WB
pRb	Human/Mouse	Santa Cruz	SC-102	AB_628209	Western blot

into the rear right flank of 6- to 8-week-old mice (n = 10 per group). Tumor volume was measured twice weekly and calculated using the equation: volume = (width^2 × length) / 2. Mice were euthanized when tumor volume reached 2,000 mm^3, as previously described (84). Animals were determined as tumor-free when no measurable tumor was observed 12 weeks post-injection. Survival curves were generated by the Kaplan-Meier method with a tumor volume of 2,000 mm^3 as an endpoint.

Statistical analysis

Data were analyzed using GraphPad Prism (San Diego, CA) and were presented as mean ± standard deviation. Statistical significance was determined using an unpaired Student's t-test. P-values <0.05 are considered statistically significant. Distributions of time-to-event outcomes (e.g., survival time) were summarized with Kaplan-Meier curves and compared across groups using the log-rank test with α = 0.01.

ACKNOWLEDGMENTS

We thank members of the Pyeon laboratory for their valuable comments and suggestions.

This work was supported by NIH R01 DE026125 and R01 DE029524 (D.P.) and the Michigan State University Global Impact Initiative (D.P.).

AUTHOR AFFILIATIONS

[1]Department of Microbiology and Molecular Genetics, Michigan State University, East Lansing, Michigan, USA
[2]Department of Molecular Biology, National Research Centre, Cairo, Egypt
[3]Philips Institute for Oral Health Research, School of Dentistry, Virginia Commonwealth University, Richmond, Virginia, USA

AUTHOR ORCIDs

Mohamed I. Khalil http://orcid.org/0000-0002-8331-1490
Iain M. Morgan https://orcid.org/0000-0002-4949-3032
Dohun Pyeon http://orcid.org/0000-0003-1970-844X

FUNDING

Funder	Grant(s)	Author(s)
HHS | National Institutes of Health (NIH)	DE026125, DE029524	Dohun Pyeon
MSU | College of Human Medicine, Michigan State University (CHM)	Global Impact Initiative	Dohun Pyeon

AUTHOR CONTRIBUTIONS

Mohamed I. Khalil, Conceptualization, Data curation, Formal analysis, Investigation, Methodology, Project administration, Resources, Software, Supervision, Validation, Visualization, Writing – original draft, Writing – review and editing | Canchai Yang, Formal analysis, Investigation, Methodology, Resources, Validation | Lexi Vu, Formal analysis, Investigation, Methodology, Software, Validation, Writing – review and editing | Smriti Chadha, Investigation | Harrison Nabors, Investigation | Claire D. James, Resources, Writing – review and editing | Iain M. Morgan, Resources, Writing – review and editing | Dohun Pyeon, Conceptualization, Formal analysis, Funding acquisition, Investigation, Project administration, Resources, Software, Supervision, Visualization, Writing – original draft, Writing – review and editing

ETHICS APPROVAL

The Michigan State University Institutional Animal Care and Use Committee (IACUC) approved experiments by National Institutes of Health guidelines for using live animals.

REFERENCES

1. Burd EM. 2003. Human papillomavirus and cervical cancer. Clin Microbiol Rev 16:1–17. https://doi.org/10.1128/CMR.16.1.1-17.2003
2. Pyeon D, Newton MA, Lambert PF, den Boon JA, Sengupta S, Marsit CJ, Woodworth CD, Connor JP, Haugen TH, Smith EM, Kelsey KT, Turek LP, Ahlquist P. 2007. Fundamental differences in cell cycle deregulation in human papillomavirus-positive and human papillomavirus-negative head/neck and cervical cancers. Cancer Res 67:4605–4619. https://doi.org/10.1158/0008-5472.CAN-06-3619
3. Griffin LM, Cicchini L, Pyeon D. 2013. Human papillomavirus infection is inhibited by host autophagy in primary human keratinocytes. Virol 437:12–19. https://doi.org/10.1016/j.virol.2012.12.004
4. Mesri EA, Feitelson MA, Munger K. 2014. Human viral oncogenesis: a cancer hallmarks analysis. Cell Host Microbe 15:266–282. https://doi.org/10.1016/j.chom.2014.02.011
5. Jabbar SF, Abrams L, Glick A, Lambert PF. 2009. Persistence of high-grade cervical dysplasia and cervical cancer requires the continuous expression of the human papillomavirus type 16 E7 oncogene. Cancer Res 69:4407–4414. https://doi.org/10.1158/0008-5472.CAN-09-0023
6. Jabbar SF, Park S, Schweizer J, Berard-Bergery M, Pitot HC, Lee D, Lambert PF. 2012. Cervical cancers require the continuous expression of the human papillomavirus type 16 E7 oncoprotein even in the presence of the viral E6 oncoprotein. Cancer Res 72:4008–4016. https://doi.org/10.1158/0008-5472.CAN-11-3085
7. Chang JTC, Kuo TF, Chen YJ, Chiu CC, Lu YC, Li HF, Shen CR, Cheng AJ. 2010. Highly potent and specific siRNAs against E6 or E7 genes of HPV16- or HPV18-infected cervical cancers. Cancer Gene Ther 17:827–836. https://doi.org/10.1038/cgt.2010.38
8. Pim D, Thomas M, Javier R, Gardiol D, Banks L. 2000. HPV E6 targeted degradation of the discs large protein: evidence for the involvement of a novel ubiquitin ligase. Oncogene 19:719–725. https://doi.org/10.1038/sj.onc.1203374
9. Gao Q, Kumar A, Singh L, Huibregtse JM, Beaudenon S, Srinivasan S, Wazer DE, Band H, Band V. 2002. Human papillomavirus E6-induced degradation of E6TP1 is mediated by E6AP ubiquitin ligase. Cancer Res 62:3315–3321.
10. White EA, Sowa ME, Tan MJA, Jeudy S, Hayes SD, Santha S, Münger K, Harper JW, Howley PM. 2012. Systematic identification of interactions between host cell proteins and E7 oncoproteins from diverse human papillomaviruses. Proc Natl Acad Sci USA 109:E260–E267. https://doi.org/10.1073/pnas.1116776109
11. Niebler M, Qian X, Höfler D, Kogosov V, Kaewprag J, Kaufmann AM, Ly R, Böhmer G, Zawatzky R, Rösl F, Rincon-Orozco B. 2013. Post-translational control of IL-1β via the human papillomavirus type 16 E6 oncoprotein: a novel mechanism of innate immune escape mediated by the E3-ubiquitin ligase E6-AP and P53. PLoS Pathog 9:e1003536. https://doi.org/10.1371/journal.ppat.1003536
12. Westrich JA, Warren CJ, Klausner MJ, Guo K, Liu C-W, Santiago ML, Pyeon D. 2018. Human papillomavirus 16 E7 stabilizes APOBEC3A protein by inhibiting cullin 2-dependent protein degradation. J Virol 92:e01318-17. https://doi.org/10.1128/JVI.01318-17
13. Huh K, Zhou X, Hayakawa H, Cho JY, Libermann TA, Jin J, Harper JW, Munger K. 2007. Human papillomavirus type 16 E7 oncoprotein associates with the cullin 2 ubiquitin ligase complex, which contributes to degradation of the retinoblastoma tumor suppressor. J Virol 81:9737–9747. https://doi.org/10.1128/JVI.00881-07
14. White EA, Münger K, Howley PM. 2016. High-risk human papillomavirus E7 proteins target PTPN14 for degradation. mBio 7:e01530-16. https://doi.org/10.1128/mBio.01530-16
15. Zhang B, Chen W, Roman A. 2006. The E7 proteins of low- and high-risk human papillomaviruses share the ability to target the pRB family member p130 for degradation. Proc Natl Acad Sci USA 103:437–442. https://doi.org/10.1073/pnas.0510012103
16. Szalmás A, Tomaić V, Basukala O, Massimi P, Mittal S, Kónya J, Banks L. 2017. The PTPN14 tumor suppressor is a degradation target of human papillomavirus E7. J Virol 91:e00057-17. https://doi.org/10.1128/JVI.00057-17
17. Oh KJ, Kalinina A, Wang J, Nakayama K, Nakayama KI, Bagchi S. 2004. The papillomavirus E7 oncoprotein is ubiquitinated by UbcH7 and cullin 1- and Skp2-containing E3 ligase. J Virol 78:5338–5346. https://doi.org/10.1128/jvi.78.10.5338-5346.2004
18. Yu ZK, Gervais JL, Zhang H. 1998. Human CUL-1 associates with the SKP1/SKP2 complex and regulates p21(CIP1/WAF1) and cyclin D proteins. Proc Natl Acad Sci USA 95:11324–11329. https://doi.org/10.1073/pnas.95.19.11324
19. Tsvetkov LM, Yeh KH, Lee SJ, Sun H, Zhang H. 1999. p27(Kip1) ubiquitination and degradation is regulated by the SCF(Skp2) complex through phosphorylated Thr187 in p27. Curr Biol 9:661–664. https://doi.org/10.1016/s0960-9822(99)80290-5
20. Ohta T, Xiong Y. 2001. Phosphorylation- and Skp1-independent *in vitro* ubiquitination of E2F1 by multiple ROC-cullin ligases. Cancer Res 61:1347–1353.
21. Deshaies RJ. 1999. SCF and cullin/ring H2-based ubiquitin ligases. Annu Rev Cell Dev Biol 15:435–467. https://doi.org/10.1146/annurev.cellbio.15.1.435
22. Alpi AF, Chaugule V, Walden H. 2016. Mechanism and disease association of E2-conjugating enzymes: lessons from UBE2T and UBE2L3. Biochem J 473:3401–3419. https://doi.org/10.1042/-BCJ20160028
23. Zhang X, Huo C, Liu Y, Su R, Zhao Y, Li Y. 2022. Mechanism and disease association with a ubiquitin conjugating E2 enzyme: UBE2L3. Front Immunol 13:793610. https://doi.org/10.3389/fimmu.2022.793610
24. Selvey LA, Dunn LA, Tindle RW, Park DS, Frazer IH. 1994. Human papillomavirus (HPV) type 18 E7 protein is a short-lived steroid-inducible

phosphoprotein in HPV-transformed cell lines. J Gen Virol 75 (Pt 7):1647–1653. https://doi.org/10.1099/0022-1317-75-7-1647
25. Lin CH, Chang HS, Yu WCY. 2008. USP11 stabilizes HPV-16E7 and further modulates the E7 biological activity. J Biol Chem 283:15681–15688. https://doi.org/10.1074/jbc.M708278200
26. Liang YJ, Chang HS, Wang CY, Yu WCY. 2008. DYRK1A stabilizes HPV16E7 oncoprotein through phosphorylation of the threonine 5 and threonine 7 residues. Int J Biochem Cell Biol 40:2431–2441. https://doi.org/10.1016/j.biocel.2008.04.003
27. Singh S, Bano A, Saraya A, Das P, Sharma R. 2021. iTRAQ-based analysis for the identification of MARCH8 targets in human esophageal squamous cell carcinoma. J Proteomics 236:104125. https://doi.org/10.1016/j.jprot.2021.104125
28. Eyster CA, Cole NB, Petersen S, Viswanathan K, Früh K, Donaldson JG. 2011. MARCH ubiquitin ligases alter the itinerary of clathrin-independent cargo from recycling to degradation. Mol Biol Cell 22:3218–3230. https://doi.org/10.1091/mbc.E10-11-0874
29. Jahnke M, Trowsdale J, Kelly AP. 2012. Ubiquitination of human leukocyte antigen (HLA)-DM by different membrane-associated RING-CH (MARCH) protein family E3 ligases targets different endocytic pathways. J Biol Chem 287:7256–7264. https://doi.org/10.1074/jbc.M111.305961
30. Chen R, Li M, Zhang Y, Zhou Q, Shu H-B. 2012. The E3 ubiquitin ligase MARCH8 negatively regulates IL-1β-induced NF-κB activation by targeting the IL1RAP coreceptor for ubiquitination and degradation. Proc Natl Acad Sci USA 109:14128–14133. https://doi.org/10.1073/pnas.1205246109
31. Khalil MI, Yang C, Vu L, Chadha S, Nabors H, Welbon C, James CD, Morgan IM, Spanos WC, Pyeon D. 2023. HPV Upregulates Marchf8 Ubiquitin Ligase and inhibits apoptosis by degrading the death receptors in head and neck cancer. PLoS Pathog 19:e1011171. https://doi.org/10.1371/journal.ppat.1011171
32. Jones DL, Alani RM, Münger K. 1997. The human papillomavirus E7 oncoprotein can uncouple cellular differentiation and proliferation in human keratinocytes by abrogating p21Cip1-mediated inhibition of cdk2. Genes Dev 11:2101–2111. https://doi.org/10.1101/gad.11.16.2101
33. McLaughlin-Drubin ME, Münger K. 2009. The human papillomavirus E7 oncoprotein. Virol 384:335–344. https://doi.org/10.1016/j.virol.2008.10.006
34. Spanos WC, Nowicki P, Lee DW, Hoover A, Hostager B, Gupta A, Anderson ME, Lee JH. 2009. Immune response during therapy with cisplatin or radiation for human papillomavirus-related head and neck cancer. Arch Otolaryngol Head Neck Surg 135:1137–1146. https://doi.org/10.1001/archoto.2009.159
35. Flores ER, Allen-Hoffmann BL, Lee D, Lambert PF. 2000. The human papillomavirus type 16 E7 oncogene is required for the productive stage of the viral life cycle. J Virol 74:6622–6631. https://doi.org/10.1128/jvi.74.14.6622-6631.2000
36. Strati K, Lambert PF. 2007. Role of Rb-dependent and Rb-independent functions of papillomavirus E7 oncogene in head and neck cancer. Cancer Res 67:11585–11593. https://doi.org/10.1158/0008-5472.CAN-07-3007
37. Shin MK, Balsitis S, Brake T, Lambert PF. 2009. Human papillomavirus E7 oncoprotein overrides the tumor suppressor activity of p21Cip1 in cervical carcinogenesis. Cancer Res 69:5656–5663. https://doi.org/10.1158/0008-5472.CAN-08-3711
38. den Boon JA, Pyeon D, Wang SS, Horswill M, Schiffman M, Sherman M, Zuna RE, Wang Z, Hewitt SM, Pearson R, Schott M, Chung L, He Q, Lambert P, Walker J, Newton MA, Wentzensen N, Ahlquist P. 2015. Molecular transitions from papillomavirus infection to cervical precancer and cancer: role of stromal estrogen receptor signaling. Proc Natl Acad Sci USA 112:E3255–E3264. https://doi.org/10.1073/pnas.1509322112
39. Trejo-Cerro O, Massimi P, Broniarczyk J, Myers M, Banks L. 2022. Repression of memo1, a novel target of human papillomavirus type 16 E7, increases cell proliferation in cervical cancer cells. J Virol 96:e0122922. https://doi.org/10.1128/jvi.01229-22
40. Seavey SE, Holubar M, Saucedo LJ, Perry ME. 1999. The E7 oncoprotein of human papillomavirus type 16 stabilizes p53 through a mechanism independent of p19(ARF). J Virol 73:7590–7598. https://doi.org/10.1128/JVI.73.9.7590-7598.1999
41. Jian Y, Schmidt-Grimminger DC, Chien WM, Wu X, Broker TR, Chow LT. 1998. Post-transcriptional induction of p21cip1 protein by human papillomavirus E7 inhibits unscheduled DNA synthesis reactivated in differentiated keratinocytes. Oncogene 17:2027–2038. https://doi.org/10.1038/sj.onc.1202142
42. Nakamura M, Bodily JM, Beglin M, Kyo S, Inoue M, Laimins LA. 2009. Hypoxia-specific stabilization of HIF-1alpha by human papillomaviruses. Virol 387:442–448. https://doi.org/10.1016/j.virol.2009.02.036
43. Smotkin D, Wettstein FO. 1987. The major human papillomavirus protein in cervical cancers is a cytoplasmic phosphoprotein. J Virol 61:1686–1689. https://doi.org/10.1128/JVI.61.5.1686-1689.1987
44. Reinstein E, Scheffner M, Oren M, Ciechanover A, Schwartz A. 2000. Degradation of the E7 human papillomavirus oncoprotein by the ubiquitin-proteasome system: targeting via ubiquitination of the N-terminal residue. Oncogene 19:5944–5950. https://doi.org/10.1038/sj.onc.1203989
45. Breitschopf K, Bengal E, Ziv T, Admon A, Ciechanover A. 1998. A novel site for ubiquitination: the N-terminal residue, and not internal lysines of myod, is essential for conjugation and degradation of the protein. EMBO J 17:5964–5973. https://doi.org/10.1093/emboj/17.20.5964
46. Aviel S, Winberg G, Massucci M, Ciechanover A. 2000. Degradation of the epstein-barr virus latent membrane protein 1 (LMP1) by the ubiquitin-proteasome pathway. targeting via ubiquitination of the N-terminal residue. J Biol Chem 275:23491–23499. https://doi.org/10.1074/jbc.M002052200
47. Poirson J, Biquand E, Straub M-L, Cassonnet P, Nominé Y, Jones L, van der Werf S, Travé G, Zanier K, Jacob Y, Demeret C, Masson M. 2017. Mapping the interactome of HPV E6 and E7 oncoproteins with the ubiquitin-proteasome system. FEBS J 284:3171–3201. https://doi.org/10.1111/febs.14193
48. Xia C, Xiao C, Luk HY, Chan PKS, Boon SS. 2023. The ubiquitin specific protease 7 stabilizes HPV16E7 to promote HPV-mediated carcinogenesis. Cell Mol Life Sci 80:278. https://doi.org/10.1007/s00018-023-04941-2
49. Ajiro M, Zheng ZM. 2015. E6^E7, a novel splice Isoform protein of human papillomavirus 16, stabilizes viral E6 and E7 oncoproteins via HSP90 and GRP78. mBio 6:e02068-14. https://doi.org/10.1128/mBio.02068-14
50. Vats A, Trejo-Cerro O, Massimi P, Banks L. 2022. Regulation of HPV E7 stability by E6-associated protein (E6AP). J Virol 96:e0066322. https://doi.org/10.1128/jvi.00663-22
51. Zheng N, Schulman BA, Song L, Miller JJ, Jeffrey PD, Wang P, Chu C, Koepp DM, Elledge SJ, Pagano M, Conaway RC, Conaway JW, Harper JW, Pavletich NP. 2002. Structure of the Cul1-Rbx1-Skp1-F boxSkp2 SCF ubiquitin ligase complex. Nature 416:703–709. https://doi.org/10.1038/416703a
52. Kamura T, Hara T, Kotoshiba S, Yada M, Ishida N, Imaki H, Hatakeyama S, Nakayama K, Nakayama KI. 2003. Degradation of p57Kip2 mediated by SCFSkp2-dependent ubiquitylation. Proc Natl Acad Sci USA 100:10231–10236. https://doi.org/10.1073/pnas.1831009100
53. Nakayama KI, Nakayama K. 2006. Ubiquitin ligases: cell-cycle control and cancer. Nat Rev Cancer 6:369–381. https://doi.org/10.1038/nrc1881
54. Wang W, Chen Y, Deng J, Zhou J, Gu X, Tang Y, Zhang G, Tan Y, Ge Z, Huang Y, Wang S, Zhou J, Zhou Y, Zhou S. 2015. Cullin1 is a novel prognostic marker and regulates the cell proliferation and metastasis in colorectal cancer. J Cancer Res Clin Oncol 141:1603–1612. https://doi.org/10.1007/s00432-015-1931-4
55. Liu W, Wang Y, Zhang C, Huang B, Bai J, Tian L. 2015. Cullin1 is up-regulated and associated with poor patients' survival in hepatocellular carcinoma. Int J Clin Exp Pathol 8:4001–4007.
56. Ping JG, Wang F, Pu JX, Hou PF, Chen YS, Bai J, Zheng JN. 2016. The expression of cullin1 is increased in renal cell carcinoma and promotes cancer cell proliferation, migration, and invasion. Tumour Biol 37:12823–12831. https://doi.org/10.1007/s13277-016-5151-6
57. Bai J, Yong HM, Chen FF, Mei PJ, Liu H, Li C, Pan ZQ, Wu YP, Zheng JN. 2013. Cullin1 is a novel marker of poor prognosis and a potential therapeutic target in human breast cancer. Ann Oncol 24:2016–2022. https://doi.org/10.1093/annonc/mdt147
58. Bai J, Zhou Y, Chen G, Zeng J, Ding J, Tan Y, Zhou J, Li G. 2011. Overexpression of cullin1 is associated with poor prognosis of patients with gastric cancer. Hum Pathol 42:375–383. https://doi.org/10.1016/j.humpath.2010.09.003

59. Chen G, Li G. 2010. Increased Cul1 expression promotes melanoma cell proliferation through regulating p27 expression. Int J Oncol 37:1339–1344. https://doi.org/10.3892/ijo_00000786
60. Qie S, Majumder M, Mackiewicz K, Howley BV, Peterson YK, Howe PH, Palanisamy V, Diehl JA. 2017. Fbxo4-mediated degradation of Fxr1 suppresses tumorigenesis in head and neck squamous cell carcinoma. Nat Commun 8:1534. https://doi.org/10.1038/s41467-017-01199-8
61. Huang L, Kinnucan E, Wang G, Beaudenon S, Howley PM, Huibregtse JM, Pavletich NP. 1999. Structure of an E6Ap-UbcH7 complex: insights into ubiquitination by the E2-E3 enzyme cascade. Sci 286:1321–1326. https://doi.org/10.1126/science.286.5443.1321
62. Arellano-Gutiérrez CV, Quintas-Granados LI, Cortés H, González Del Carmen M, Leyva-Gómez G, Bustamante-Montes LP, Rodríguez-Morales M, López-Reyes I, Padilla-Mendoza JR, Rodríguez-Páez L, Figueroa-González G, Reyes-Hernández OD. 2022. Indole-3-Carbinol, a phytochemical aryl hydrocarbon receptor-ligand, induces the mRNA overexpression of UBE2L3 and cell proliferation arrest. Curr Issues Mol Biol 44:2054–2068. https://doi.org/10.3390/cimb44050139
63. Flores-Pérez A, Elizondo G. 2018. Apoptosis induction and inhibition of hela cell proliferation by alpha-naphthoflavone and resveratrol are aryl hydrocarbon receptor-independent. Chem Biol Interact 281:98–105. https://doi.org/10.1016/j.cbi.2017.12.029
64. Ma X, Zhao J, Yang F, Liu H, Qi W. 2017. Ubiquitin conjugating enzyme E2 L3 promoted tumor growth of NSCLC through accelerating p27kip1 ubiquitination and degradation. Oncotarget 8:84193–84203. https://doi.org/10.18632/oncotarget.20449
65. Ma X, Qi W, Yang F, Pan H. 2022. UBE2L3 promotes lung adenocarcinoma invasion and metastasis through the GSK-3/snail signaling pathway. Am J Transl Res 14:4549–4561.
66. Yu C, Liu Q, Zhao Z, Zhai J, Xue M, Tang Y-D, Wang C, Zheng C, Blanco-Melo D. 2023. The emerging roles of MARCH8 in viral infections: a double-edged sword. PLoS Pathog 19:e1011619. https://doi.org/10.1371/journal.ppat.1011619
67. Barouch-Bentov R, Neveu G, Xiao F, Beer M, Bekerman E, Schor S, Campbell J, Boonyaratanakornkit J, Lindenbach B, Lu A, Jacob Y, Einav S. 2016. Hepatitis C virus proteins interact with the endosomal sorting complex required for transport (ESCRT) machinery via ubiquitination to facilitate viral envelopment. mBio 7:e01456-16. https://doi.org/10.1128/mBio.01456-16
68. Kumar S, Barouch-Bentov R, Xiao F, Schor S, Pu S, Biquand E, Lu A, Lindenbach BD, Jacob Y, Demeret C, Einav S. 2019. MARCH8 ubiquitinates the Hepatitis C virus nonstructural 2 protein and mediates viral envelopment. Cell Rep 26:1800–1814. https://doi.org/10.1016/j.celrep.2019.01.075
69. Roy N, Pacini G, Berlioz-Torrent C, Janvier K. 2017. Characterization of E3 ligases involved in lysosomal sorting of the HIV-1 restriction factor BST2. J Cell Sci 130:1596–1611. https://doi.org/10.1242/jcs.195412
70. Tada T, Zhang Y, Koyama T, Tobiume M, Tsunetsugu-Yokota Y, Yamaoka S, Fujita H, Tokunaga K. 2015. MARCH8 inhibits HIV-1 infection by reducing virion incorporation of envelope glycoproteins. Nat Med 21:1502–1507. https://doi.org/10.1038/nm.3956
71. Zhang Y, Tada T, Ozono S, Kishigami S, Fujita H, Tokunaga K. 2020. MARCH8 inhibits viral infection by two different mechanisms. elife 9:e57763. https://doi.org/10.7554/eLife.57763
72. Zhang Y, Ozono S, Tada T, Tobiume M, Kameoka M, Kishigami S, Fujita H, Tokunaga K, Kalia M. 2022. MARCH8 targets cytoplasmic lysine residues of various viral envelope glycoproteins. Microbiol Spectr 10:e0061821. https://doi.org/10.1128/spectrum.00618-21
73. Villalón-Letelier F, Brooks AG, Londrigan SL, Reading PC. 2021. MARCH8 restricts influenza A virus infectivity but does not downregulate viral glycoprotein expression at the surface of infected cells. mBio 12:e0148421. https://doi.org/10.1128/mBio.01484-21
74. Liu X, Xu F, Ren L, Zhao F, Huang Y, Wei L, Wang Y, Wang C, Fan Z, Mei S, Song J, Zhao Z, Cen S, Liang C, Wang J, Guo F. 2021. MARCH8 inhibits influenza A virus infection by targeting viral M2 protein for ubiquitination-dependent degradation in lysosomes. Nat Commun 12:4427. https://doi.org/10.1038/s41467-021-24724-2
75. Ludwig S, Marczak L, Sharma P, Abramowicz A, Gawin M, Widlak P, Whiteside TL, Pietrowska M. 2019. Proteomes of exosomes from HPV(+) or HPV(-) head and neck cancer cells: differential enrichment in immunoregulatory proteins. Oncoimmunol 8:1593808. https://doi.org/10.1080/2162402X.2019.1593808
76. Ayuso JM, Vitek R, Swick AD, Skala MC, Wisinski KB, Kimple RJ, Lambert PF, Beebe DJ. 2019. Effects of culture method on response to EGFR therapy in head and neck squamous cell carcinoma cells. Sci Rep 9:12480. https://doi.org/10.1038/s41598-019-48764-3
77. Ou D, Wu Y, Zhang J, Liu J, Liu Z, Shao M, Guo X, Cui S. 2022. miR-340-5p affects oral squamous cell carcinoma (OSCC) cells proliferation and invasion by targeting endoplasmic reticulum stress proteins. Eur J Pharmacol 920:174820. https://doi.org/10.1016/j.ejphar.2022.174820
78. Kume T, Deng K, Hogan BL. 2000. Minimal phenotype of mice homozygous for a null mutation in the forkhead/winged helix gene, Mf2. Mol Cell Biol 20:1419–1425. https://doi.org/10.1128/MCB.20.4.1419-1425.2000
79. Evans MR, James CD, Bristol ML, Nulton TJ, Wang X, Kaur N, White EA, Windle B, Morgan IM. 2019. Human papillomavirus 16 E2 regulates keratinocyte gene expression relevant to cancer and the viral life cycle. J Virol 93:e01067-19. https://doi.org/10.1128/JVI.01067-19
80. James CD, Prabhakar AT, Otoa R, Evans MR, Wang X, Bristol ML, Zhang K, Li R, Morgan IM, Laimins LA. 2019. SAMHD1 regulates human papillomavirus 16-induced cell proliferation and viral replication during differentiation of keratinocytes. mSphere 4:e00448-19. https://doi.org/10.1128/mSphere.00448-19
81. Allen-Hoffmann BL, Schlosser SJ, Ivarie CA, Sattler CA, Meisner LF, O'Connor SL. 2000. Normal growth and differentiation in a spontaneously immortalized near-diploid human keratinocyte cell line, NIKS. J Invest Dermatol 114:444–455. https://doi.org/10.1046/j.1523-1747.2000.00869.x
82. Labun K, Montague TG, Krause M, Torres Cleuren YN, Tjeldnes H, Valen E. 2019. CHOPCHOP v3: expanding the CRISPR web toolbox beyond genome editing. Nucleic Acids Res 47:W171–W174. https://doi.org/10.1093/nar/gkz365
83. Warren CJ, Xu T, Guo K, Griffin LM, Westrich JA, Lee D, Lambert PF, Santiago ML, Pyeon D. 2015. APOBEC3A functions as a restriction factor of human papillomavirus. J Virol 89:688–702. https://doi.org/10.1128/JVI.02383-14
84. Cicchini L, Westrich JA, Xu T, Vermeer DW, Berger JN, Clambey ET, Lee D, Song JI, Lambert PF, Greer RO, Lee JH, Pyeon D. 2016. Suppression of antitumor immune responses by human papillomavirus through epigenetic downregulation of CXCL14. mBio 7:e00270-16. https://doi.org/10.1128/mBio.00270-16